IG 42-GM DC MOTOR SYSTEM ANALYSIS USING LQR AND LQT METHODS

Dwi Rizky Anto[1], Alwy Muhammad Ravi[2], Khayla Shafa Syahira[2], Anggara Trisna Nugraha[3,4,*]

[1]*Department of Marine Electrical Engineering, Shipbuilding Institute of Polytechnic Surabaya, Indonesia*
Jl. Teknik Kimia, Kampus ITS Sukolilo, Sukolilo, Surabaya, Jawa Timur, Indonesia
[1]dwirizky@student.ppns.ac.id

[2] *Electrical Engineering Study Program, School of Electrical Engineering, Telkom University, Indonesia*
Jl. Telekomunikasi No. 1, Terusan Buah Batu, Sukapura, Kec. Dayeuhkolot, Kabupaten Bandung, Jawa Barat 40257
[2]alwymuhammadravi@telkomuniversity.ac.id, [2]khaylashafas@student.telkomuniversity.ac.id

[3]*Department of Bio-industrial Mechatronics Engineering, National Chung Hsing University, Taiwan*
No. 145, Xingda Rd., South Dist., Taichung City 402, Taiwan

[4] *Associate Degree Department of Marine Electrical Engineering, Shipbuilding Institute of Polytechnic Surabaya, Indonesia*
Jl. Teknik Kimia, Kampus ITS Sukolilo, Sukolilo, Surabaya, Jawa Timur, Indonesia
[4]anggaranugraha@ppns.ac.id

Article history:

Received May 19, 2026
Revised June 22, 2026
Accepted July 20, 2026
Available online August 4, 2026

Keywords:

DC Motor Speed, Linear Quadratic Regulator, Linear Quadratic Tracking, Matlab, Mathematical Model, Optimal control.

Abstract

DC motors are extensively employed across di verse industrial applications due to their versatility in both fixed and variable-speed electric drives spanning wide power ranges. This study investigates the transient response characteristics of a separately excited DC motor speed control system using the Linear Quadratic Regulator (LQR) and Linear Quadratic Tracking (LQT) methods, with LQT parameters optimized via a Genetic Algorithm (GA). The IG 42-GM DC motor was modelled using first-order transfer functions and simulated in MATLAB/Simulink. Simulation results demonstrate that under noise-free conditions, both LQR and LQT achieve the intended setpoint of 1.0 with no undershoot. Under noisy conditions, LQR maintains a setpoint output of 1.0 with a controlled undershoot of 0.5, while LQT achieves the setpoint with irregular waveform responses due to noise interference. These findings confirm the effectiveness of LQR and GA-optimized LQT strategies for robust, cost-efficient DC motor speed control in variable power-rating systems.

I. INTRODUCTION

Technological advancement is currently progressing at an unprecedented pace, influencing every facet of modern life. It is evident that the contemporary demand for technology far exceeds that of previous decades, a reality that has intensified global competition, particularly within the automation sector (Gebremariam & Alemu, 2023). In this competitive landscape, industry players are actively constructing or upgrading their industrial systems to produce superior products relative to their competitors, while others prioritize manufacturing speed. This drive for efficiency and performance has led to the widespread

[*] Corresponding author

adoption of the electric motor, which is essential for industrial progress. Market reports indicate that the electric motor market continues to expand, and the Asia-Pacific region accounts for a major share of sales (Asia Pacific Electric Motor Market Size Report, 2023; Asia Pacific Electric Motor Sales Market Size & Outlook, 2022; Asia Pacific Electric Motor Market Size, Share & Growth, 2024). This data underscores the critical role of electric motors, particularly DC motors, in determining both production speed and quality.

Despite their widespread use, the application of DC motors in industrial settings is often challenged by difficulties in torque control (Kumar & Thilagar, 2015). Researchers have consistently noted that the torque variable in DC motors is inherently difficult to measure directly, often necessitating its estimation (Antar et al., 2023). This challenge is compounded by the fact that DC motors exhibit non-linear behavior, especially when subjected to varying loads. While conventional controllers, such as Proportional-Integral-Derivative (PID) controllers, are widely used due to their established performance in linear systems, their efficacy is significantly compromised in non-linear environments (Urrea-Quintero et al., 2021).

In response to these challenges, this paper presents a control system for induction motors utilizing a PID controller integrated with the Field-Oriented Control (FOC) method. This approach is designed to enhance the torque current control signal within the PID controller framework (Kasula et al., 2023). Furthermore, optimal control techniques, such as the Linear Quadratic Regulator (LQR), have been employed by several researchers (Zhi et al., 2022). In this study, a permanent magnet DC motor is used as the plant for identification and control via the LQR optimal control technique. To facilitate this, a DC motor identification module has been developed using Simulink-Matlab.

The performance of the LQR is highly dependent on the appropriate selection of the state weighting matrix (Q) and the control weighting matrix (R), which directly determine the feedback gain values and performance indices (da Silva et al., 2024). While a manual tuning (trial-and-error) approach can be used, it often yields sub-optimal results (Youns et al., 2013). Consequently, this study employs a Genetic Algorithm (GA) to automate and optimize the selection of the Q and R matrices (da Silva et al., 2024; Robandi et al., 2001). The integration of GA with LQR has been shown to significantly improve control performance compared to traditional methods, offering a more efficient and effective solution for complex control problems (Gebremariam & Alemu, 2023; Youns et al., 2013).

II. Related Works

Several studies have investigated optimal control strategies for DC motor systems. Gebremariam and Alemu (2023) conducted a comprehensive review of DC motor drive control schemes and optimization techniques, highlighting that conventional fixed-gain controllers are increasingly being replaced by intelligent and optimal control methods due to their superior adaptability in industrial automation environments. Their review established the growing importance of advanced control strategies, particularly in applications where speed regulation and load disturbance rejection are critical.

In the context of LQR-based control, Zhi et al. (2021) proposed an interval linear quadratic regulator for DC motor speed control under parametric uncertainties, demonstrating that LQR-based methods provide stronger robustness and faster response speed compared to traditional PID controllers, particularly when system parameters vary during operation.

Regarding the optimization of LQR weighting matrices, Youns et al. (2013) proposed the integration of Genetic Algorithm (GA) with LQR for DC motor control, showing that GA-optimized Q and R matrices yield significantly better transient response and reduced steady-state error compared to manual trial-and-error tuning. This finding was further reinforced by da Silva et al. (2024), who confirmed that the GA-LQR combination offers a systematic and efficient framework for balancing control expenditure and system performance in dynamic systems.

Building on these works, the present study applies both LQR and Linear Quadratic Tracking (LQT) methods to the IG 42-GM DC motor using MATLAB/Simulink, with GA employed to optimize the Q and R matrices, extending prior research by incorporating trajectory tracking capability alongside regulation performance.

III. Methods

3.1 Transfer Function

The transfer function helps in analyzing the features of a system. In general, the structure of a first-order system can be expressed as follows:

$$G(s) = \frac{K}{cs + 1} \quad (1)$$

The general form of a second-order system can be expressed in the following standard form:

$$G(s) = \frac{\omega n^2}{s^2 + 2\varsigma\omega n s + \omega n^2} \quad (2)$$

3.2 Linear Quadratic Regulator

The Linear Quadratic Regulator (LQR) constitutes a fundamental method within modern control theory (Zhi et al., 2022). Analysis of systems employing LQR is conducted using the state-space representation, a framework particularly well-suited for multi-input multi-output (MIMO) systems due to its mathematical simplicity. The widespread application of LQR across various domains has led to the extensive utilization of its design techniques (Bagua, 2023).

Equation 2 presents a block diagram of a DC motor control system incorporating an LQR controller. In such a configuration, the motor speed may vary in response to changes in load and other external disturbances. The primary function of the LQR is to minimize deviations in motor speed (Umar & Upadhyay, 2024). The system output, specifically the motor speed, is continuously compared with the applied input, namely the motor voltage. The reduction of motor speed deviations is executed by the LQR.

$$\begin{aligned} x &= Ax + Bu \\ y &= Cx \end{aligned} \quad (3)$$

The performance index based on minimum energy (cost function/quadratic function) is given by Equation (2).

$$J = \frac{1}{2}\int_0^\infty (x^T Q + u^T R u)dt \quad (4)$$

The regulator equation can be solved by solving the Riccati algebraic equation as given in Equations (5)–(7).

$$A^T P + PA - PBR^{-1}B^T + Q = 0 \quad (5)$$
$$-K = R^{-1}B^T P \quad (6)$$
$$u = -Kx \quad (7)$$

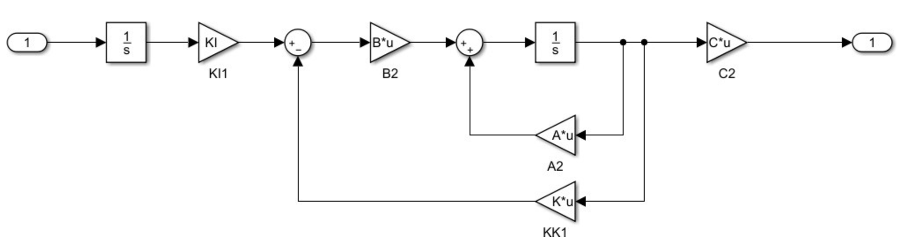

Figure 1. Modelling of a Linear Quadratic Regulator

Figure 1 illustrates the fundamental closed-loop configuration of a DC motor speed control system. The reference speed (setpoint) is compared with the actual motor speed measured by a tachometer or encoder. The error signal is processed by a controller (LQR/LQT) that generates a control voltage applied to the DC motor via a power amplifier. This configuration enables precise speed regulation despite load variations and external disturbances.

3.3 Linear Quadratic Tracking

Linear Quadratic Tracking is a linear control system in which the system output follows a desired reference trajectory (Aghazamani et al., 2022). system has the state equation (3) and an error vector as shown in Equation (4). The performance index is defined in Equation (5).

$$e = z - y \tag{8}$$

$$J = \frac{1}{2}e'(t_f)F(t_f)e(t_f) + \frac{1}{2}\int_{t_0}^{t_f}[e''Qe + U'Ru]dt \tag{9}$$

Once the mathematical model of the system is represented in state-space form, the solution matrix for the Riccati differential equation can be determined using Equation (10) in the case of infinite time.

$$0 = -PA - A'P + PBR^{-1}B'P + C'QC \tag{10}$$

The matrix Q and R can be selected to fit the system's intended performance. Once the Riccati equation has been obtained, the non-homogeneous vector differential equation can be derived using Equation (11).

$$g = -[A - BR^{-1}B'P]'g - C'Qz \tag{11}$$

Once the matrix P which is a positive-definite symmetric matrix and g have been obtained, the feedback gain K can be calculated using Equation (12).

$$K = R^{-1}B'P \tag{12}$$

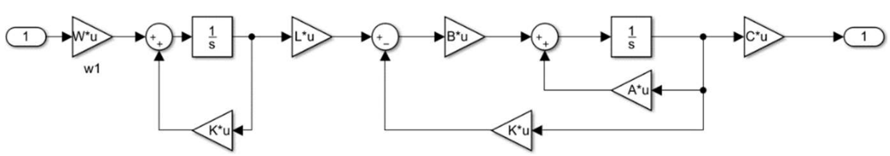

Figure 2. Modelling of a Linear Quadratic Tracking

Figure 2 presents the block diagram of an LQT control system. Unlike LQR which drives the state to zero, LQT enables the system output y to track a time-varying reference trajectory z. The error signal $e=z-y$ feeds into the performance index minimization. The Riccati equation (Equation 10) and non-homogeneous vector differential equation (Equation 11) are solved to compute the optimal feedback gain K and feedforward gain, ensuring asymptotic tracking with minimal control effort.

3.4 Noise

In communication systems, noise refers to unwanted signals that are always present in a transmission system (Uzor-Ejikeme, 2023). This noise degrades the quality of the desired signal and ultimately disrupts the process of data transmission and reception (Xie et al., 2022; Xu et al., 2023).

3.5 Modelling of DC Motors

3.5.1 First-Order LQR DC Motor

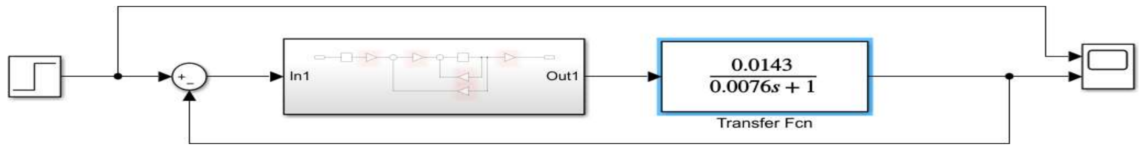

Figure 3. LQR First-Order Modelling of a DC Motor

Figure 3 shows the Simulink implementation of a first-order LQR controller for the IG 42-GM DC motor. The first-order transfer function $G(s)$=0.0143/(0.0076s+1) is derived from the motor datasheet. The LQR block computes the optimal control gain K from the state-space matrices A, B, C, and the weighting matrices Q and R. The control law $u=-Kx$ minimizes the quadratic cost function, producing a smooth speed response with zero steady-state error.

3.5.2 First-Order LQT DC Motor

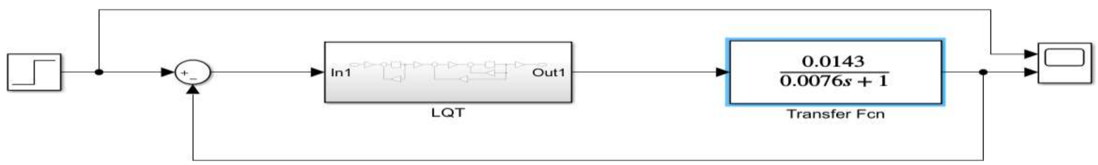

Figure 4. LQT First-Order Modelling of a DC Motor

Figure 4 depicts the first-order LQT Simulink model for the IG 42-GM DC motor. Unlike LQR, the LQT configuration incorporates a reference trajectory input, enabling the system output to follow a desired setpoint trajectory. The tracking error is integrated into the performance index minimization, and the MATLAB function solves the algebraic Riccati equation to produce the feedback gain matrix $K = R^{-1}B^{T}P$. Simulation results show that LQT achieves the intended setpoint of 1.0 under both noise-free and noisy conditions, with no undershoot observed in either scenario.

3.5.3 First-Order LQR DC Motor with Noise

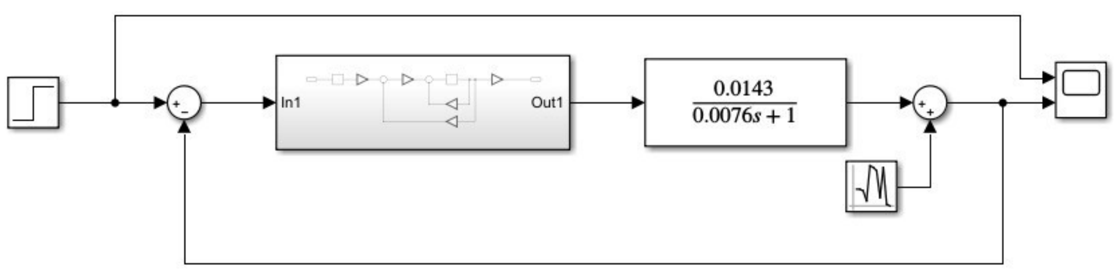

Figure 5. LQR First-Order Modelling of a DC Motor with Noise

Figure 5 illustrates the first-order LQR model with additive noise injected into the system. The noise block simulates real-world electrical interference, sensor noise, or load disturbances commonly present in industrial DC motor environments. The LQR controller demonstrates robustness by maintaining the setpoint output at 1.0 despite the presence of noise, although the waveform becomes irregular. This confirms LQR's disturbance rejection capability under non-ideal operating conditions.

3.5.4 First-Order LQT DC Motor with Noise

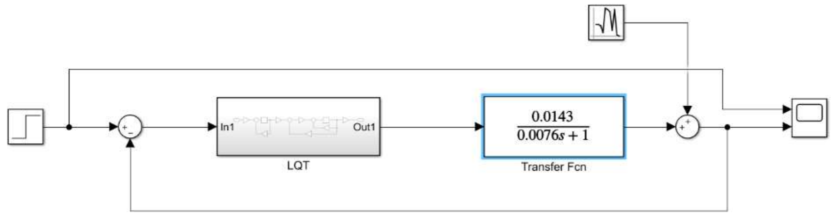

Figure 6. LQT First-Order Modelling of a DC Motor with Noise

Figure 6 presents the LQT model under noisy conditions. The injection of noise into the feedback path simulates real-world measurement uncertainties. Simulation results (Table 2) indicate that LQT with noise maintains the intended setpoint of 1.0; however, the additional noise input produces an irregular waveform response. This suggests that LQT is more sensitive to high-frequency noise compared to LQR, requiring additional filtering or higher weighting on control effort (R) to improve noise immunity.

GEARED MOTOR TORQUE/SPEED

	減速比 Reduction ratio	1/4	1/14	1/17	1/24	1/49	1/61	1/84	1/104	1/144	1/212	1/294	1/504	1/624	1/720	1/864	1/1062	1/1470	1/2500	1/3000	1/3600
12V	定格扭力(Kg-cm) Rated torque	2.2	6.5	8.1	10	18	18	18	20	20	25	25	30	30	30	30	30	30	30	30	30
	定格回轉數(rpm) Rated speed	1400	405	325	248	120	98	76	63	45	31	24	13.5	10.9	9.5	8.0	6.5	4.6	2.7	2.3	1.9
24V	定格扭力(Kg-cm) Rated torque	1.8	5.4	6.6	9.5	18	18	18	20	20	25	25	30	30	30	30	30	30	30	30	30
	定格回轉數(rpm) Rated speed	1445	420	340	240	122	102	77.5	63	47	31	23.8	13.5	10.9	9.5	8.0	6.5	4.6	2.7	2.3	1.9

馬達單體型式 /MOTOR DATA

定格電壓 Rated volt (V)	定格扭力 Rated torque (g-cm)	定格回轉數 Rated speed (rpm)	定格電流 Rated current (mA)	無負荷回轉數 No load speed (rpm)	無負荷電流 No load current (mA)	定格出力 Rated output (W)	重量 Weight (g)
12	700	5700	≤ 5500	7000	≤ 900	41.3	360
24	570	5900	≤ 2100	7000	≤ 500	34.7	360

Figure 7. Specifications of the IG 42-GM DC Motor

Figure 7 displays the key electromechanical specifications of the IG 42-GM DC motor used in this study. The torque constant (τ=78g/cm=0.0076N/m) and current rating (I=0.53A) are highlighted. These parameters are essential for deriving the first-order transfer function, where the DC motor coefficient $K=\tau/I$=0.0143. Additional parameters include moment of inertia J=110.25g·cm^2, damping ratio b=2.2, resistance R=22.641Ω, and inductance L=0.000325H, all of which are used in the state-space representation (Equations 3 and 8).

- τ = 78g/cm = 0,0076 N/m
- Rated Current = 530 mA = 0,53 A
- Voltage = 12V
- Rated Speed = 5290 rpm = 553.96 m/s
- ς = 2,2
- Resistance = 22,641 ohm
- Inductance = 0.000325 H
- Momen of Inertia $= \frac{1}{2}\ x\ m(R1^2 + R2^2)$

$$= \frac{1}{2}\ x\ 0{,}36(17{,}5^2 + 17{,}5^2)$$

$$= 110{,}25\ kg\backslash m^2$$

3.6 First- and Second-Order Mathematical Models

3.6.1 First-Order

General form of a first-order transfer function

$$G(s) = \frac{K}{cs + 1} \tag{13}$$

First-Order DC Motor Based on the DC motor datasheet, the following first-order equation is obtained: Where $r = K.\, i$, so that

$$K \;=\; \frac{c}{i} \;=\; \frac{0{,}0076}{0{,}53} \;=\; 0{,}0143 \tag{14}$$

Note:
K = DC motor coefficient
r = DC motor torque
I = DC motor current
Thus, the first-order equation for a DC motor is obtained:

$$G(s) = \frac{0{,}0143}{0{,}0076s} \tag{15}$$

3.6.2 Second-Order

The general form of a second-order transfer function is as follows:

$$G(s) = \frac{\omega n^2}{s^2 + 2\varsigma \omega n s + \omega n^2} \tag{16}$$

Based on the DC motor datasheet, the following second-order equation for the DC motor is obtained:

$$G(s) = \frac{(314)^2}{s^2 + 2(16)(314)s + (314)^2} \tag{17}$$

$$G(s) = \frac{98596}{s^2 + 10048s + 9859} \tag{18}$$

Note:

ωn = Natural Frequency

ς = Damping Ratio

3.7 MATLAB Script for a Linear Quadratic Regulator

```
% OPTIMASI SISTEM LQR PADA MOTOR DC
clear;
clc;
% Model Motor DC IG 42-GM
J = 110.25    ; b= 2.2 ; K= 0.0196 ; R= 22.641 ; L = 0.000325 ;
% J = Momeninesia , b = Rasioredam, K= konstanta, R= resistansi, L=
% Induktansi
A = [-b/J K/J; -K/L -R/L];
```

```
B = [0; 1/L];
C = [1 0]

AA = [ A zeros(2,1); -C 0];
BB = [B;0];

% Pole Placement
J = [-3 -4 -5];
K = acker(AA,BB,J);
KI = -K(3);
KK = [K(1) K(2)];

% MatrixLQR
Q = [1 0 0;
     0 1 0;
     0 0 1000];
R = [1];

K_lqr = lqr(AA,BB,Q,R)
KI2 = -K_lqr(3);
KK2 = [K_lqr(1) K_lqr(2)];
```

3.8 MATLAB Script for a Linear Quadratic Tracking

```
% OPTIMASI SISTEM LQT PADA MOTOR DC
clear;
clc;
% Model Motor DC IG 42-GM
J = 110.25    ; b= 2.2 ; K= 0.0196 ; R= 22.641 ; L = 0.000325 ;
% J = Momeninersia , b = Rasioredam, K= konstanta, R= resistansi, L=Induktansi
A = [-b/J K/J; -K/L -R/L]; %A
B = [0; 1/L]; %B
C = [1 0] %C

Q=10; R=0.0000000001; %0.00000000000001 \\KI
W=C'*Q; %KK

[S,o,m,n]=care(A,B,C'*Q*C,R) %m=v(t) %S=P
K=inv(R)*B'*S %feedback Gain
ACL=(A-B*K)'
L=inv(R)*B' %model following gain
```

IV. RESULTS AND DISCUSSIONS

The input and output values for the Linear Quadratic Regulator and Linear Quadratic Tracking techniques are displayed in the simulation results. Because the MATLAB Simulink circuits utilised in each experiment are distinct, each experiment produces a new set of findings. In certain MATLAB results, the values surpass the calculation limitations, making it impossible to ascertain the precise simulation results; in other noise-based simulations, the graphs are challenging to understand due to the wide range of simulation inputs.

Notes:
A = TUK SISO
B = TUK SISO with NOISE

4.1 Results of DC Motor Simulation

Tabel 1. Results of the LQR and LQT Simulations

Methods	*Scope*	Without Noise	
		Set Point	*Undershoot*
LQR		1	-
LQT		1	-

The output of the first-order LQR DC motor hits the intended set point, but the first-order LQT DC motor does not, according to the oscilloscope's data. The step input values are shown on the blue graphs. The output of the first-order LQR and LQT DC motors is shown on the orange graph.

4.2 Simulation Results for a DC Motor with Noise

It is evident from the oscilloscope findings that the output of the first-order LQR and LQT systems for this DC motor noise meets the intended set point; nevertheless, further input noise results in an irregular waveform. For this DC motor noise, the orange waveform shows the output of the first-order LQR and LQT systems, while the blue waveform shows the step input.

Tabel 2. Simulation Results for a DC Motor with Noise.

Metode	*Scope*	With Noise	
		Set Point	*Undershoot*
LQR	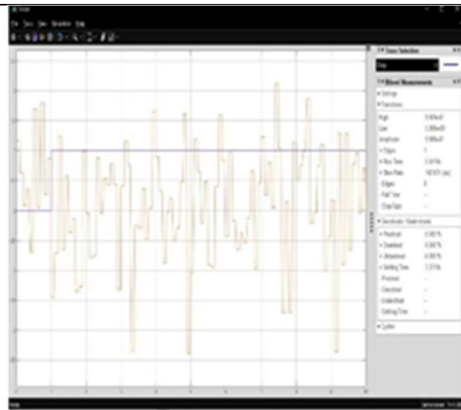	1	0,5
LQT	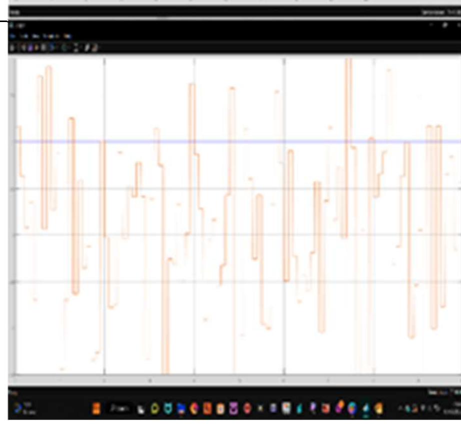	1	-

V. Conclusions And Recommendations

The step response of the LQR and LQT systems for a DC motor must be determined using the transfer function obtained from the first-order modelling of the DC motor when running Simulink simulations in MATLAB. A supporting DC motor datasheet is needed in order to receive the first-order DC motor's mathematical model. The IG 42-GM DC motor datasheet was utilised in this experiment. The intended set-point output of 1 and a 0.5 undershoot in the LQR noise were obtained from the simulation results for the LQR and LQT systems utilising the transfer function from the first-order mathematical model of the IG 42-GM DC motor with noise.

Acknowledgments

M. R. A. A. thanks the Department of Marine Electrical Engineering Technology, Shipbuilding Institute of Polytechnic Surabaya (PPNS), Surabaya, Indonesia, for providing the facilities and academic support that enabled the completion of this research.

References

Gebremariam, S. F., & Alemu, B. S. (2023). A Review on DC Motor Drive Controlling Schemes, Optimization Techniques and Future Trends. *International Journal of Research Publication and Reviews, 4*(12), 271-285. https://doi.org/10.55248/gengpi.4.1223.0127.

Fortune Business Insights. (2024). Asia Pacific electric motor market size, share & COVID-19 impact analysis (Report

No. FBI113323). https://www.fortunebusinessinsights.com/asia-pacific-electric-motor-market-113323.

Grand View Research. (2024). Asia Pacific electric motor sales market size & outlook, 2030. Grand View Research. https://www.grandviewresearch.com/horizon/outlook/electric-motor-sales-market/asia-pacific.

KBV Research. (2023, November). Asia Pacific electric motor market size, share & industry trends analysis report by output power, by type, by end user, by country and growth forecast, 2023–2030 (Report No. KBV-18562). https://www.kbvresearch.com/asia-pacific-electric-motor-market/.

Kumar, S., & Thilagar, S. (2015). Sensorless Load Torque Estimation and Passivity Based Control of Buck Converter Fed DC Motor. The Scientific World Journal, 2015. https://doi.org/10.1155/2015/132843.

Antar, R. K., Saleh, A. A., & Yahia, T. T. (2023). Estimate and control speed of a DC motor using different power circuits. Przegląd Elektrotechniczny, 99(3). https://doi.org/10.15199/48.2023.03.48.

Urrea-Quintero, J., Fuhg, J., Marino, M., & Fau, A. (2021). PI/PID controller stabilizing sets of uncertain nonlinear systems: an efficient surrogate model-based approach. Nonlinear Dynamics, 105, 277 - 299. https://doi.org/10.1007/s11071-021-06431-1.

Firdaus, AA, Sobhita, RA and Nugraha, AT. "Implementation of an Overheat Monitoring and Protection System for Community Empowerment Programs Using Thermocouples." Maritime in Community Service and Empowerment 3.1, 2025,

Fatqurrochman, MI, Nugraha, AT and Sobhita, RA. "Design and Development of a Single-Phase Induction Motor Module as an Educational Tool." Maritime in Community Service and Empowerment 3.1, 2025,

Rohman, YF, Nugraha, AT and Sobhita, RA. "Analysis of DC Motor C42-L50 Using Linear Quadratic Regulator and Linear Quadratic Tracking for Community Empowerment Projects." Maritime in Community Service and Empowerment 3.1, 2025,

Rohman, YF, Nugraha, AT and Sobhita, RA. "Converter as a Voltage Output Stabilizer for Wind Turbines." Journal of Electrical, Marine and Its Application 3.1, 2025,

Sunarno, E, Nugraha, AT and Sobhita, RA. "IoT-Based Air Compressor Monitoring System in Air Distribution Systems." Journal of Electrical, Marine and Its Application 3.1, 2025,

Jamaludin, M, Sobhita, RA and Nugraha, AT. "Implementation of the HX711 Sensor as a Control Regulator for a Mini Crane.." Journal of Electrical, Marine and Its Application 3.1, 2025,

Pradana, SY, Hazim, A and Nugraha, AT. "Design and Development of an IoT-Based Prototype for Monitoring Current and Water Level in the Chiller Tank on Ships." Journal of Electrical, Marine and Its Application 3.1, 2025,

Fatqurrochman, MI and Nugraha, AT. "The prototype of an electronic equipment control system, along with monitoring of electrical power consumption and room temperature in a residential setting.." Journal of Electrical, Marine and Its Application 3.1, 2025,

Nugraha, AT and Sobhita, RA. "Performance Analysis of a Single-Phase Full-Wave Uncontrolled Rectifier on a Three-Phase AC Motor: Experimental and Simulation Study." Journal of Electrical, Marine and Its Application 3.1, 2025,

Juniani, AI, Nugraha, AT, Setiawan, E, Amelia, P, Handandi, ZZ and Hidayana, E. "Enhancing water quality prediction using the decision tree approach with the C4. 5 Algorithm." JEEMECS (Journal of Electrical Engineering, Mechatronic and Computer Science …, 2025,

Nugraha, AT, Eviningsih, RP, Lesmana, SV and Sobhita, RA. "Loop Configuration Analysis of BLM57050-Type DC Motor." International Conference on Applied Science and Technology on Engineering …, 2025,

Oktaviano, R, Nugraha, AT and Jami'in, MA. "Study Perbandingan Pemodelan Orde 1 dan Orde 2 pada Motor DC RS-775SH-8013 dan Motor AC 1 Phasa Havells 1.5 HP." Conference of Electrical, Marine and Its Application 4.1, 2025,

Saputra, FY. "Representasi Matematis dan Simulasi Sistem Dinamik Motor DC054B-6." Conference of Electrical, Marine and Its Application 4.1, 2025,

Fatqurrochman, MI, Saputra, DE and Nugraha, AT. "Performance Analysis of C23-L54 Series DC Motors in K3 System Using LQR Tracking Controller for Improved Operational Efficiency and Safety."

Journal of Safety, Health, and Environmental Engineering 3.2, 2025, pp. 1-9.,

Hati, IJP, Nugraha, AT and Jami'in, MA. "Pemodelan dan Simulasi Dinamik Motor DC Brushless BN23HS-28HS 02 dan Motor AC Satu Fasa SIMTACH AC040M-08J30A Berbasis MATLAB/Simulink." Conference of Electrical, Marine and Its Application 4.1, 2025,

Fauzi, AR, Nugraha, AT and Jami'in, MA. "Permodelan Matematis Orde Satu dan Orde Dua Motor DC Maxon RE 50 Berdasarkan Step Response." Conference of Electrical, Marine and Its Application 4.1, 2025,

Rahmatullah, RMN, Nugraha, AT and Jami'in, MA. "Permodelan Matematis Sistem Motor DC MOOG C34-L70 Orde Satu dan Orde Dua." Conference of Electrical, Marine and Its Application 4.1, 2025,

Pratama, MST, Nugraha, AT and Jami'in, MA. "Permodelan Elektromekanis dan Analisis Fungsi Alih Motor DC Maxon DCX 35 L untuk Sistem Kontrol Presisi." Conference of Electrical, Marine and Its Application 4.1, 2025,

Ardiansyah, MD, Nugraha, AT and Jami'in, MA. "Perbandingan Respons Sistem Motor DC dan Motor AC Berdasarkan Identifikasi Model Menggunakan MATLAB/Simulink." Conference of Electrical, Marine and Its Application 4.1, 2025,

Lesmana, SV, Nugraha, AT, Jamaludin, M and Sobhita, RA. "Sistem Kontrol LQR dan PID pada Mesin Pengering Biji Kopi." Seminar MASTER PPNS 10.1, 2025, pp. 251-261.,

Uzor-Ejikeme, C. (2023). Noise and interference in transmission of speech signals in the corporate network. In Information Security: Proceedings of the 59th Scientific Conference of Postgraduates, Master's Students and Students of BSUIR (pp. 173–175). Belarusian State University of Informatics and Radioelectronics. https://libeldoc.bsuir.by/handle/123456789/51982.

Xie, N., Xiong, W., Chen, J., Zhang, P., Huang, L., & Su, J. (2022). Multiple phase noises physical-layer authentication. IEEE Transactions on Communications, 70(9), 6196–6211. https://doi.org/10.1109/TCOMM.2022.3195925.

Xu, H., Wang, L., & Zhang, Q. (2023). Signal-to-noise ratio degradation analysis for optoelectronic feedback-based chaotic optical communication https://doi.org/10.1364/OL.497061.